Article

Pulsed Field Gradient NMR Studies of Polymer Adsorption on Colloidal CdSe Quantum Dots

Lei Shen, Ronald Soong, Mingfeng Wang, Anna Lee, Chi Wu, Gregory D. Scholes, Peter M. Macdonald, and Mitchell A. Winnik

J. Phys. Chem. B, **2008**, 112 (6), 1626-1633 • DOI: 10.1021/jp0768975

Pulsed Field Gradient NMR Studies of Polymer Adsorption on Colloidal CdSe Quantum Dots

Lei Shen,[†,‡] Ronald Soong,[†,§] Mingfeng Wang,[†] Anna Lee,[†] Chi Wu,[‡,||] Gregory D. Scholes,[†] Peter M. Macdonald,*[,†,§] and Mitchell A. Winnik*[,†]

Department of Chemistry, University of Toronto, 80 St. George Street, Toronto, M5S 3H6 Ontario, Canada, The Hefei National Laboratory for Physical Sciences at Microscale, Department of Chemical Physics, University of Science and Technology of China, Hefei, Anhui 230026, China, Department of Chemical and Physical Sciences, University of Toronto Mississauga, 3359 Mississauga Road, Mississauga, L5L 1C6 Ontario, Canada, and Department of Chemistry, The Chinese University of Hong Kong, Shatin, N.T., Hong Kong

Received: August 28, 2007; In Final Form: November 1, 2007

Pulsed field gradient nuclear magnetic resonance (PFG NMR) experiments have been used to examine ligand exchange between poly(2-(*N*,*N*-dimethylamino)ethyl methacrylate) (PDMA) ($M_n = 12\,000$, $M_w/M_n = 1.20$, $N_n = 78$) and trioctylphosphine oxide (TOPO) bound to the surface of CdSe/TOPO quantum dots (QDs). We show that PFG ^{1}H NMR can quantify the displacement of TOPO by PDMA through its ability to differentiate signals due to TOPO bound to the QDs versus those from TOPO molecules free in solution. For CdSe QDs with a band edge absorption maximum at 558 nm (diameter 2.7 nm by transmission electron microscopy), we determined that, at saturation, 8 polymer chains on average displace greater than 90% of the surface TOPO groups. At partial saturation, with an average of 6 polymer chains/QD, each TOPO displaced requires 28 DMA repeat units. Assuming that one Me_2N- group binds to a surface Cd^{2+} for each TOPO displaced, we infer that only about 3% of the DMA units are directly bound to the surface. The remaining groups are present as loops or tails that protrude into the solvent and increase the hydrodynamic diameter of the particles.

Introduction

Fluorescent colloidal semiconductor nanocrystals, also known as quantum dots (QDs), are the subject of intense research because their size-dependent optical properties lead to applications in novel linear and nonlinear optical devices,[1−8] in catalysis,[9−11] and as biological tags.[12−14] These materials are normally synthesized by an organometallic route involving high temperature and consist of an inorganic core surrounded by a shell of capping ligands. These ligands, which consist of a polar head groups and an organic tail, serve three main functions. First, the polar head group passivates the surface of the QDs and can lead to material with high photoluminescent quantum efficiencies. Second, the organic tail provides colloidal stability in solution, preventing aggregation and growth. Finally, functional groups associated with the tail can serve as sites for binding the QDs to surfaces or the covalent attachment of biomolecules. The incorporation of QDs into devices or into biological systems often requires strategies for the manipulation of the ligands bound to the QD surface to make them water-soluble and biocompatible.

While many research groups have used ligand exchange as an approach to modifying the properties of colloidal QDs, the tools for studying the exchange process remain limited. This is particularly true for the case in which one uses the pendant groups of polymers as multidentate ligands for these QDs.[15−17] Polymers can provide robust colloidal stability over a broad range of solvents. They can carry ionic or reactive functional groups for incorporation into end-use applications. A wide range of different homopolymers and copolymers are amenable to synthesis, providing a wide scope for ligand engineering. Thus, there is an urgent need for better tools to study the interaction of polymers with colloidal QDs solutions.

In this paper, we explore the use of pulsed field gradient ^{1}H NMR (PFG NMR)[18] to study polymer−ligand exchange for CdSe QDs prepared in the presence of a mixture of trioctylphosphine (TOP) and trioctylphosphine oxide (TOPO) after purification to remove excess ligand. These QDs often have photoluminescence (PL) quantum yields in the range 2−8% and limited long-term stability, due to slow ligand dissociation accompanied by particle aggregation. Because of difficulties in distinguishing between the ^{1}H NMR resonances of TOPO and TOP associated with the QDs, we will refer to the material as CdSe/TOPO, keeping in mind that the particle surface may also contain TOP ligands. In the past, we have shown the polymer poly(2-(*N*,*N*-dimethylamino)ethyl methacrylate) (PDMA) undergoes ligand exchange with CdSe/TOPO in toluene solution to yield CdSe/PDMA with very different solubility properties.[17] The polymer renders the particles soluble in a variety of polar organic solvents (ketones, alcohols such as methanol, toluene, and tetrahydrofuran (THF)) but insoluble in simple alkanes, which are effective at dissolving CdSe/TOPO. The polymer can also lead to an increase in PL quantum yield, but that is not a topic of consideration in this report. A curious feature of the CdSe/PDMA particles is that they do not form colloidal solutions in water, even though PDMA itself is soluble in water. While there may be several reasons for this behavior, one

* To whom correspondence should be addressed. E-mail: mwinnik@chem.utoronto.ca (M.A.W.); pm.macdonald@utoronto.ca (P.M.M).
† University of Toronto.
‡ University of Science and Technology of China.
§ University of Toronto Mississauga.
|| The Chinese University of Hong Kong.

10.1021/jp0768975 CCC: $40.75
Published on Web 01/18/2008

possibility is that some tightly bound TOPO ligands, which can be detected by ^{1}H NMR, render portions of the surface hydrophobic. This problem can be overcome by the use of multiple exchanges and a more hydrophilic polymer, a poly(ethylene glycol)−PDMA diblock copolymer.[17d]

An important challenge is to determine the amount of polymer bound to the particle surface. In 2006, we published a report[17c] showing that this information could be obtained using size exclusion chromatography (SEC) if the polymer contained a single chromophore at one end. The SEC column can separate the colloidal QDs from unbound polymer, and adding known amounts of QDs to a well-defined polymer solution with a small excess of polymer led to a decrease in the peak area for the polymer that could be interpreted quantitatively. In this way, we learned that CdSe/TOPO QDs with a diameter of 4.0 nm could bind on average 12 molecules of PDMA of $M_n = 6700$, $M_w/M_n = 1.2$, and $N_n = 43$. These experiments, while effective, were cumbersome and time-consuming. Here we show that this type of quantitative information is more readily obtained using PFG NMR.

PFG NMR, as described in numerous learned reviews,[18] has been widely and successfully employed to measure the self-diffusion coefficient (D_s) in a host of circumstances, including those of colloids and polymers, whether linear, cyclic, star-branched, or rodlike. Through the Stokes−Einstein expression, $1/D_s$ is directly related to the hydrodynamic radius (R_h) in solution. PFG NMR is also attractive because it can be used for mixture analysis even in regions of the spectrum where resonances from different components overlap. For example, Johnson, Murray, and co-workers[19,20] have used diffusion-order NMR spectroscopy (DOSY), based on the PFG NMR technique, to determine the R_h of alkanethiol-stabilized gold clusters. Ribot et al.[21] investigated laurate-capped CeO_2 colloids, and Hens et al.[22a] measured D_s values of TOPO-capped InP colloids using PFG NMR. These results confirmed that PFG NMR is a plausible method to characterize the hydrodynamic dimensions of nanometer-sized metallic and semiconductor nanoparticles in solution. Hens et al.[22b] also used integration of TOPO methyl resonances of the InP/TOPO dissolved in toluene-d_8 to show that the TOPO ligands desorbed from the surface as the solution was diluted. From this information, they were able to determine the binding isotherm for the ligand on the QDs.

In this report, we describe the characterization of CdSe/TOPO QDs in chloroform-*d* solution using the PFG NMR technique. We demonstrate, first, that PFG ^{1}H NMR readily determines the dimension of different sized QDs. Second, we show that PFG ^{1}H NMR spectroscopy differentiates TOPO ligands bound to the QDs surface from those free in solution, based on their different self-diffusion coefficients. This permits us to examine quantitatively the polymer−ligand exchange process, in which linear PDMA homopolymers displace TOPO from the QDs surface. We generate, thereby, a measure of the number of DMA monomer units required to displace one TOPO from the QDs surface and the fraction of such monomer units interacting with the QDs/bound PDMA.

Experimental Section

Materials. TOPO-capped CdSe QDs (CdSe/TOPO) were prepared through an established organometallic approach at high temperature[23,24] in a mixture of trioctylphosphine (TOP) and trioctylphosphine oxide (TOPO) and purified to remove excess phosphine ligands by precipitation in methanol (ACP, 99.8%) followed by redispersion in toluene (ACP, 99.8%). One sample with a band edge adsorption at 558 nm was purified by three successive precipitation−redispersion steps, whereas two other CdSe/TOPO samples lost colloidal stability if more than one cycle was attempted. Oleic acid-capped PbS (PbS/OA) nanoparticles were prepared by the standard method as described previously.[25] The PbS/OA particles were also purified by three successive precipitation−redispersion steps using methanol and toluene. Chloroform-*d* (D, 99.8% with 0.05% v/v TMS, Cambridge Isotope Lab. Inc.) was used directly as received. Cu^{I}Br (98%, Aldrich) was washed repeatedly with acetic acid and ether and then dried and stored under nitrogen. 1,1,4,7,-10,10-Hexamethyltriethylenetetramine (HMTETA) (97%), 2-(*N*,*N*-dimethylamino)ethyl methacrylate (DMA) (98%), and triethylamine (99.5%) were purchased from Aldrich and used without further purification. The initiator 1-pyrenemethyl 2-bromoisobutyrate (Py-BIBB) was synthesized as described previously.[17c] THF was purified by distillation from sodium plus benzophenone.

Synthesis of Poly(2-(*N*,*N*-dimethylamino)ethyl methacrylate) (PDMA) Homopolymer. Cu^{I}Br (0.092 g, 0.64 mmol) and HMTETA (0.30 g, 1.28 mmol) were placed into a 50 mL Schlenk flask fitted with rubber septa and degassed by three freeze−pump−thaw cycles. In another flask DMA (6.0 g, 38.16 mmol) and Py-BIBB (0.121 g, 0.32 mmol) were mixed under stirring and purged with N_2 for 30 min to remove oxygen. The mixture was then transferred to the Schlenk flask to initiate the polymerization with a two-end needle under N_2. The polymerization was maintained at room temperature for 30 min. The mixture became very viscous, and the polymerization was terminated by immersing the flask into a liquid-N_2 bath. Then the mixture was diluted with approximate 150 mL of THF and passed through a column of basic aluminum oxide to remove the copper catalyst. After most solvent was evaporated, the rest of the solution was precipitated in *n*-hexane. The solid product was dissolved in THF again and precipitated in *n*-hexane, and this process was repeated for 4 cycles. Finally, the resulting polymer was dried at 40 °C under vacuum for 3 days. Yield: 60%. The monomer conversion was measured by gravimetry. The absolute molecular weight was obtained by end-group analysis using ^{1}H NMR ($M_n = 12\,000$). The molecular weight distribution ($M_w/M_n = 1.20$) was measured by size exclusion chromatography (SEC) with THF containing 2% triethylamine (v/v) as the eluent, and polystyrene standards were used to generate the calibration curve.

Sample Preparation. CdSe/TOPO QDs, with a band edge adsorption at 558 nm, were prepared for NMR measurements by first removing the toluene solvent under vacuum at 60 °C, followed by dissolving the dry residue in $CDCl_3$ to achieve a QDs concentration of 5 mg/mL, equivalent to 1.0×10^{-7} mol of QDs/mL. The concentration of CdSe/TOPO was calculated through the Beer−Lambert law ($c = A/(\epsilon L)$),[26] and the extinction coefficient (ϵ) of CdSe/TOPO QDs was determined by the empirical equation $\epsilon = 5857d^{2.65}$ (d is the diameter of the CdSe/TOPO QDs measured by TEM). Ligand exchange was performed in $CDCl_3$ at 20 °C by stirring a mixture of PDMA and freshly purified CdSe/TOPO for 3 days.

NMR Spectroscopy. All NMR spectra were recorded on a Varian Infinity 500 MHz NMR spectrometer using a Varian 5 mm double resonance liquids probe. All spectra were recorded at a sample temperature of 20.0 ± 0.5 °C. Proton T_1 relaxation times were measured using a standard inversion recovery protocol. Proton T_2 relaxation times were measured from the delay time dependence of the intensity in the Carr−Purcell−Meiboom−Gill (CPMG) echo experiment.

^{1}H NMR diffusion measurements were performed at 499.78 MHz using the stimulated echo (STE) pulsed field gradient (PFG) procedure,[27] with a square field gradient pulse of constant duration (δ) equal to 5 ms and a variable gradient pulse amplitude (g). The field gradient pulses were applied along the longitudinal (z) direction exclusively. Typical acquisition parameters were as follows: a 90° pulse length of 16 μs; a spin echo delay (τ_2) of 10 ms; a longitudinal delay (τ_1) of 200 ms; a recycle delay of 5 s; a spectral width of 10 kHz and a 4K data size, corresponding to an acquisition time of 1.6 s. The phases of the radio frequency pulses were cycled as described by Fauth et al.[28] to remove unwanted echoes. Spectra were processed with an exponential multiplication equivalent to 5 Hz line broadening prior to Fourier transformation and were referenced to tetramethylsilane. Gradient strength was calibrated from the known diffusion coefficient of HDO at 20 °C.[29]

Data Analysis. In the stimulated echo (STE) pulsed field gradient (PFG) NMR sequence (see Figure S1 in the Supporting Information), during the first gradient pulse of magnitude g (T/m) and duration δ (s) nuclear spins are encoded with a phase shift $\Phi = \gamma g \delta z$, where γ is the particular magnetogyric ratio and z is the spin's displacement along the direction of the applied field gradient. In the absence of diffusion during the diffusion time $\Delta = \tau_1 + \tau_2$ the second identical gradient pulse produces an equal rephasing of the magnetization and, consequently, an unattenuated echo forms. If diffusion occurs during the delay time Δ, then the rephasing is incomplete and the resulting echo is attenuated proportionately. In STE PFG NMR for the case of unrestricted isotropic diffusion of a single species the stimulated echo intensity (I) decays according to

$$I = I_0 \exp(-2\tau_2/T_2) \exp(-\tau_1/T_1) \exp[-(\gamma g \delta)^2(\Delta - \delta/3)D_s] \quad (1)$$

where D_s is the isotropic self-diffusion coefficient, while T_1 and T_2 are the longitudinal and transverse relaxation times, respectively. Experimentally, either the gradient pulse amplitude, or its duration, or the diffusion time may be incremented progressively. To extract diffusion coefficients from such experimental data the resonance intensity $\ln(I/I_0)$ is plotted versus $k = [(\gamma g \delta)^2(\Delta - \delta/3)]$ such that the diffusion coefficient corresponds to the slope. In the STE PFG NMR sequence $\Delta = \tau_1 + \tau_2$ so that for situations where $T_1 > T_2$ the experimentally accessible diffusion time is limited by T_1 rather than T_2, which confers the ability to employ longer diffusion times, thereby facilitating diffusion measurements for cases of slower diffusion, or lower gradient strengths, or lower γ nuclei.

For the case of overlapping resonances from independently diffusing species undergoing slow exchange on the time scale of the diffusion measurement, such as the TOPO free in solution and bound to the QDs surface, the diffusive decay is a sum of exponentials

$$I/I_0 = \Sigma f_i \exp(-2\tau_2/T_{2i}) \exp(-\tau_1/T_{1i}) \exp(-kD_{si}) \quad (2)$$

where f_i is the fractional intensity contributed by species i ($\Sigma f_i = 1$) having self-diffusion coefficient D_{si} and longitudinal and transverse relaxation times T_{1i} and T_{2i}, respectively.

For the purpose of fitting eq 2 to experimental data, the relaxation times of each component must be determined independently. For a two-component fit, initial estimates of the self-diffusion coefficients are obtained from the small k and large k decays, and then the overall STE PFG NMR intensity decay is simulated using eq 2, assuming initial values for the relative populations f_i. The relative populations and diffusion coefficients are then refined based on a χ^2 error analysis in which the diffusion coefficients are fixed while varying the relative populations. The diffusion coefficients are then varied iteratively until a global minimum χ^2 was obtained, with χ^2 is defined as

$$\chi^2 = [1/(N-n)] \sum_{i=1}^{N} \{[(I/I_0)_{i,\mathrm{exp}} - (I/I_0)_{i,\mathrm{calcd}}]/(I/I_0)_{i,\mathrm{exp}}\}^2 \quad (3)$$

where N is the number of different I/I_0 values and n the number of variable parameters, where typically $N = 20$ and $n = 3$.

From the diffusion coefficient one may calculate the hydrodynamic radius of the diffusing species, R_h, using the Stokes–Einstein equation

$$D_s = kT/(6\pi\eta R_h) \quad (4)$$

where k is the Boltzmann constant and η is the solution viscosity at the measuring temperature T. The viscosity is readily obtained from the same STE PFG NMR data set if the solvent, of known molecular radius, exhibits a proton resonance.

Results and Discussion

^{1}H NMR Spectra. We begin by presenting in Figure 1 the ^{1}H NMR spectrum of TOPO, CdSe/TOPO, the polymer PDMA, and a CdSe/TOPO/PDMA mixture in chloroform-*d* solution. For TOPO itself, distinct resonances a, b, and d are observed at 1.56, 1.65, and 1.38 ppm, respectively, for CH_2 protons and resonance e at 0.88 ppm for the terminal CH_3 group. The remaining CH_2 groups c yield a set of superimposed resonances at around 1.28 ppm. When bound to CdSe/TOPO QDs, these proton resonances are not significantly shifted relative to TOPO free in solution but instead are all broadened, an effect attributed to the close-packing TOPO ligands on the surface of nanoparticles.[30,31] PDMA free in chloroform-*d* solution exhibits well-resolved resonances readily assigned to particular methylene and methyl protons, as shown in Figure 1, among which the amino methyls at 2.28 ppm are especially noteworthy, as is the fact that no PDMA resonances occur in the region of the proton spectrum occupied by the TOPO methylene groups c. As shown in the bottom spectrum, when PDMA is added to CdSe/TOPO QDs, the TOPO resonance c is readily resolved from the PDMA resonances. This means that in the PFG NMR diffusion experiment it will be possible to independently and simultaneously monitor the diffusion of PDMA and TOPO.

Diffusion Coefficients and Particle Diameters. In Figure 2 we plot the decay of the STE PFG ^{1}H NMR resonance c of the TOPO methylenes for a solution of 5.0 mg/mL (1.0×10^{-4} M QDs) CdSe/TOPO in $CDCl_3$. A typical STE PFG ^{1}H NMR spectral data set from which the intensities were obtained is shown in Figure S2 in the Supporting Information. This sample, with a band-edge absorption maximum at 558 nm, had been purified of excess free TOPO by three precipitations from toluene into methanol. The linear signal decay for CdSe/TOPO is characteristic of a single diffusing species, and from the slope we calculate $D_{s(\mathrm{CdSe/TOPO})} = 2.40\ (\pm 0.05) \times 10^{-10}$ m^2/s. In a parallel experiment on TOPO free in $CDCl_3$ (not shown), we obtained $D_{s(\mathrm{TOPO})} = 7.55\ (\pm 0.05) \times 10^{-10}$ m^2/s. The lower curve in Figure 2 is the signal decay for a 5.0 mg/mL solution in $CDCl_3$ of CdSe/TOPO QDs to which an additional 2.8 mg/mL TOPO was added. One sees a nonlinear decay which can be fitted to a sum of two exponentials as per eq 2 with diffusion coefficients of 8.59×10^{-10} and 2.40×10^{-10} m^2/s, i.e., close to those of the corresponding free TOPO and CdSe/TOPO QDs.

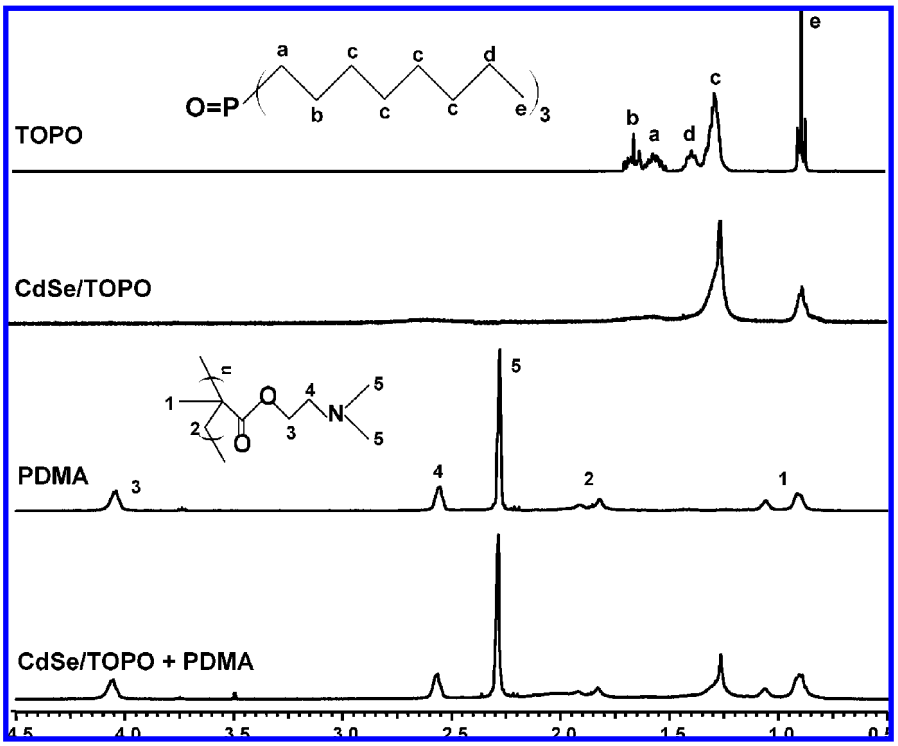

Figure 1. ^{1}H NMR spectra of TOPO molecules (4.5 mg/mL), CdSe/TOPO QDs (5.0 mg/mL), PDMA polymers (2.5 mg/mL), and CdSe/TOPO + PDMA (2:1 wt) mixtures (5.0 mg/mL for QDs) in $CDCl_3$ at 20 °C.

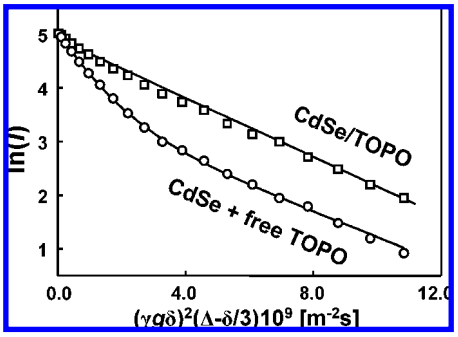

Figure 2. Stimulated echo intensity attenuation I of the TOPO NMR signal at 1.28 ppm in the STE PFG NMR diffusion experiment (20 °C, $\delta = 5$ ms, $\Delta = 210$ ms) in $CDCl_3$ as a function of the gradient strength g for CdSe/TOPO QDs (5.0 mg/mL) and CdSe/TOPO QDs (5.0 mg/mL) also containing 2.80 mg/mL free TOPO. The solid lines are the curves of best fit obtained using eq 1 for CdSe/TOPO QDs and eq 2 for CdSe + free TOPO, with relaxation times as provided in Table S1 in the Supporting Information and the fitting parameters described in the text.

From this experiment, we learn that the two TOPO populations diffuse as independent entities without exchange on the diffusion time scale (Δ) of the experiment.

The curve fitting with eq 2 requires knowledge of the individual T_1 and T_2 relaxation times. Their values measured for the purified CdSe/TOPO QDs and free TOPO are listed in Table S1 in the Supporting Information and reflect one's expectation that the TOPO mobility decreases upon binding to the QD surface. Note that the spectral acquisition conditions provide for full relaxation of the CH_2 resonances of both TOPO populations. From eq 2, using these same relaxation times, the fitted weight fractions of the two components were $f_{fast} = 0.70$ and $f_{slow} = 0.30$. Thus, the original 5.0 mg of CdSe/TOPO QDs can be calculated to contain approximately 1.2 mg of TOPO bound to the surface. This value of 24 wt % TOPO corresponds to that reported by others for similar sized CdSe/TOPO QDs. For instance, Wang et al.[17b] used peak integration of the ^{1}H NMR spectrum in the presence of an internal standard to obtain a value of 20 wt % TOPO, while Kuno et al.[32] used thermal gravimetric analysis (TGA) to obtain 23 wt % TOPO. Furthermore, given that the 1.2 mg of TOPO bound to the surface corresponds to 3.12×10^{-6} mol of TOPO ($M_r = 386$ g/mol) and that the number of QDs equals 1.0×10^{-7} mol, one estimates that one QD bears 31 TOPO.

Since concentration has little effect on the magnitude of the QD, D_s values in these PFG NMR experiments (see, for example, Figure S3 in the Supporting Information), we can employ the Stokes−Einstein equation according to eq 4 to calculate the hydrodynamic diameter ($d_h = 2R_h$) of the particles. For the CdSe/TOPO sample in $CDCl_3$ with the first absorption wavelength of 558 nm, we obtain $d_h = 3.22 \pm 0.07$ nm. The size of QD core ($d_{core} = 2.7 \pm 0.5$ nm) was determined independently by transmission electron microscopy (TEM). The size difference is due to the contribution of the TOPO capping layer on the diameter of the particles in solution. Note that, on the basis of the size of the QD core, each of the 31 TOPO molecules bound at the surfaces is estimated to occupy a surface area of roughly 8.3 Å^2.

These experiments were also repeated with two other CdSe/TOPO samples with band-edge absorption maxima at 513 and 588 nm. Here we experienced difficulty in obtaining colloidally stable samples with most of the excess TOPO removed. Samples subjected to a single precipitation in methanol gave stable colloidal solutions in $CDCl_3$ but after a second precipitation could no longer be dissolved or dispersed in toluene or $CDCl_3$. The PFG NMR decay traces for these samples resembled the lower curve in Figure 2. We could obtain the QD diffusion coefficient values from the slow decay. These, along with the d_{core} values obtained by TEM, are presented in Table 1 and confirm the expectation that the band edge emission is shifted progressively to the red as the CdSe particle core size increases.

Table 1 also includes the results of measurement on an oleic acid-capped PbS nanocrystal (PbS/OA) sample in $CDCl_3$ in

TABLE 1: Self-Diffusion Coefficient (D_s) Determined by PFG NMR and Particle Diameter (d) from PFG NMR and TEM for Different QDs with Different UV−Vis Absorption Wavelengths

QDs (λ_{max},[a] nm)	D_s[b] (10^{-10} m^2/s)	d_h[c] (nm)	d_{TEM}[d] (nm)
CdSe (513 nm)[e]	2.58 ± 0.20	3.15 ± 0.24	2.1 ± 0.5
CdSe (558 nm)	2.40 ± 0.05	3.22 ± 0.07	2.7 ± 0.5
CdSe (588 nm)[e]	1.50 ± 0.10	5.15 ± 0.34	4.5 ± 0.3
PbS (1109 nm)	1.90 ± 0.02	4.01 ± 0.04	3.5 ± 0.5

[a] Band-edge absorption wavelength of the CdSe/TOPO samples. [b] Self-diffusion coefficient obtained by PFG NMR. [c] Hydrodynamic diameter calculated from the Stokes−Einstein expression, eq 4. [d] Core diameter obtained by TEM. [e] These two samples could not be precipitated and redispersed more than once. The QD self-diffusion coefficients were obtained by fitting the PFG NMR diffusive decays of the TOPO signal using eq 2.

which the diffusion coefficient was determined by monitoring the methylene resonances of the OA ligands at 1.30 ppm. These data are included to emphasize the general utility of PFG NMR to determine the hydrodynamic diameter of QDs in solution.

Ligand Exchange with Poly(2-(*N*,*N*-dimethylamino)ethyl methacrylate) (PDMA). Ligand exchange is widely used to modify the surface properties of colloidal nanocrystals.[15,17] By proper choice of ligands, one can modify the colloidal properties of the nanoparticles and introduce functional groups for the covalent attachment of photoactive or electroactive species. We have a particular interest in using polymers with functional pendant groups as multidentate ligands for QDs.[17] Polymer−QDs interactions are a special case of polymer−colloid interactions, a topic with a long history that has been extensively studied, both experimentally and theoretically.[33] Nevertheless, relatively little is known about the interaction of polymers with particles as small as typical QDs. Most of our experiments have been carried out on low-to-medium molar mass samples of PDMA. We have, for example, shown that PDMA interacts with TOPO-passivated CdSe, ZnSe, and core/shell CdSe/ZnS QDs in toluene or $CHCl_3$ to provide colloidally robust nanoparticles that form colloidal solutions in a variety of polar and semipolar solvents such as alcohols, acetonitrile, *N*-methylpyrrolidone (NMP), and tetrahydrofuran (THF) but are insoluble in nonpolar solvents like hexane.[17] ^{31}P NMR experiments demonstrate that the polymer displaces TOPO from the particle surface to generate free TOPO molecules in solution.[15,17] Unfortunately, the ^{31}P NMR experiment is not quantitative, and sometimes the peaks due to free TOPO are too weak to be observed.

Here, we use the STE PFG NMR technique to monitor polymer binding and ligand exchange of CdSe/TOPO and PDMA. The QDs sample employed is the sample shown in Figure 2 (purified by three precipitation−redispersion cycles) with a band-edge emission at 558 nm. The PDMA sample (M_n = 12 000, M_w/M_n = 1.20, and a number average degree of polymerization N_n = 78) was synthesized by atom-transfer radical polymerization (ATRP) as described in the Experimental Section. To investigate the ligand exchange process, a small amount of PDMA polymer (5.0 mg, 4.2×10^{-7} mol) was added to 1.0 mL of a $CDCl_3$ solution of CdSe/TOPO QDs (5.0 mg/mL, 1.0×10^{-4} M). The number ratio of polymer to QDs is 4:1. From previous experiments,[17] we anticipated that this represented less than the full amount of PDMA that could bind to these QDs. The mixtures were stirred for 3 days to promote equilibration.

In Figure 3 we compare the STE PFG ^{1}H NMR signal decay for the PDMA dimethylamino resonance at 2.28 ppm (upper line) with that of the TOPO CH_2 resonance c at 1.28 ppm (lower line). The straight line for the PDMA resonance suggests a

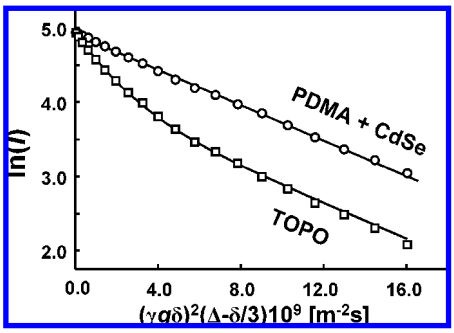

Figure 3. Stimulated echo intensity attenuation I of the NMR signal for QDs (5.0 mg/mL, 1.0×10^{-4} M) at 1.28 ppm and PDMA (5.0 mg/mL, 4.2×10^{-4} M) at 2.28 ppm in the STE PFG NMR diffusion experiment (20 °C, δ = 5 ms) of PDMA/QDs mixture $CDCl_3$ solution as a function of the gradient strength g with Δ = 310 ms. The solid lines are the curves of best fit obtained using eq 1 for CdSe/PDMA and eq 2 for TOPO, with relaxation times as provided in Table S1 in the Supporting Information and the fitting parameters described in the text.

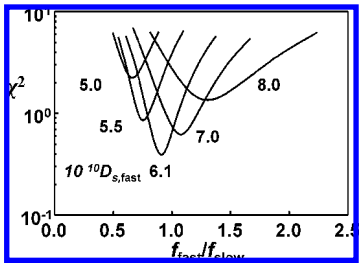

Figure 4. Plot of χ^2 vs f_{fast}/f_{slow} for various assumed values of $D_{s,fast}$ indicated in the figure for the data presented in the lower curve in Figure 3. The optimum fit corresponds to the minimum value of χ^2.

situation characterized by a single diffusion coefficient. The PDMA diffusion coefficient here is close to, but not identical with, that characteristic of free PDMA in $CDCl_3$ (see Figure 5, below). The two values are too similar, however, to allow a differentiation of PDMA free in solution from PDMA bound to QDs on the basis of their relative diffusion coefficients alone. Such a differentiation might well be possible with a lower molecular weight PDMA polymer. Note, as well, that the largest PDMA ^{1}H NMR resonance, which arises from the amino methyl protons, shows no significant difference in line width between PDMA free in solution and bound to QDs.

The lower line in Figure 3, monitored at peak c of TOPO, is curved but can be fitted as a sum of two exponentials, as per eq 2, indicating that TOPO exists as two independently diffusing populations. The slow TOPO decay has the same slope as the PDMA decay. We infer that this slope describes the diffusion of QDs that contain both PDMA and TOPO bound to the CdSe surface. The fast decay corresponds to the diffusion of TOPO molecules that have been displaced from the QDs. Optimum fitting parameters were obtained by examination of the χ^2 surface (eq 3) for combinations of the fitting parameters D_s and f_{fast} (f_{slow} = 1 − f_{fast}) that led to the smallest mean-squared differences between the fitted and experimental data. An example is shown in Figure 4 for the fitting of the lower curve in Figure 3, where it is evident that the best fit is obtained for the fitting parameters $D_{s,slow} = 1.9 \times 10^{-10}$ m^2 s^{-1}, $D_{s,fast} = 6.1 \times 10^{-10}$ m^2 s^{-1}, and f_{fast}/f_{slow} = 0.90. The fact that these diffusion coefficients so closely correspond with those of TOPO free in solution (see below) and TOPO bound to the CdSe surface as in Figure 2 indicates that the ratio f_{fast}/f_{slow} = 0.90 defines the fraction of TOPO that has been displaced from the CdSe particle surface by PDMA.

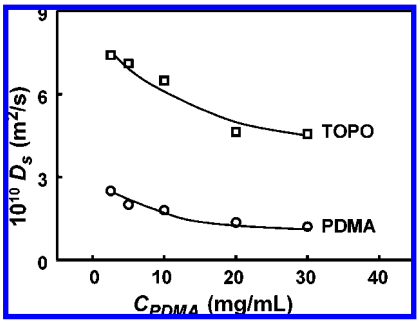

Figure 5. Self-diffusion coefficients (D_s) of PDMA and TOPO (2.5 mg/mL) components as a function of PDMA concentration in $CDCl_3$ at 20 °C.

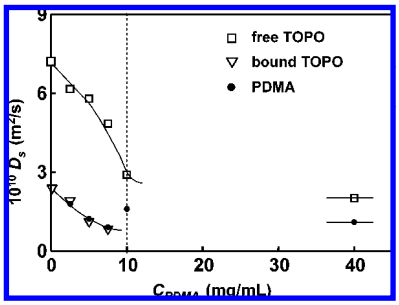

Figure 6. Self-diffusion coefficients of PDMA and TOPO as a function of PDMA concentration in $CDCl_3$ with CdSe QDs (5.0 mg/mL) at 20 °C. When the concentration of PDMA is below 10.0 mg/mL, both fast and slow TOPO components can be observed. Free TOPO refers to the fast component and bound TOPO refers to the slow component. When the concentration of PDMA is 10.0 mg/mL or greater, only one mode of TOPO diffusion can be observed.

Values of $D_{s,fast}$ obtained in this way vary with the concentration of PDMA added and do not correspond to the value obtained for TOPO itself in $CDCl_3$. These results suggest that there are subtle features of TOPO diffusion in the presence of PDMA that need to be elucidated. The upper line of Figure 5 shows a plot of the measured diffusion coefficients of TOPO (2.5 mg/mL in $CDCl_3$) as a function of increasing concentrations of PDMA. The lower line shows the corresponding diffusion coefficients for PDMA itself. Both values decrease with increasing PDMA concentration. The decrease in D_{PDMA} is likely due to a small concentration-dependent increase in monomeric friction coefficient, which is often seen in PFG NMR studies of polymer in dilute solution. We focus on the even more pronounced decrease in D_{TOPO}. The fact that D_{CDCl_3} (not shown) hardly changes indicates that there are no significant changes in solution viscosity over this range of polymer concentration fractions. As an alternative explanation, we propose a weak interaction between TOPO and PDMA that leads to a TOPO−polymer complex in rapid equilibrium with free TOPO:

$$\text{TOPO} + \text{PDMA} \leftrightarrow \text{TOPO}-\text{PDMA} \qquad (5)$$

The complex would presumably have mobility comparable to that of the polymer. Because of the rapid exchange, one would measure a signal decay that represented a weighted average of the fraction of bound TOPO and the mobility of the two species. We use this argument to rationalize the slower decay of TOPO in the presence of free PDMA and in the presence of TOPO-covered QDs.

Figure 6 shows the results of the analysis of PFG NMR experiments in which we added incrementally increasing amounts of PDMA to solutions of CdSe/TOPO (5.0 mg/mL) in $CDCl_3$. For concentrations of PDMA below 10 mg/mL, we obtained plots similar to those shown in Figure 3, i.e., monoexponential for PDMA and biexponential for TOPO. For the TOPO signal, the $D_{s,slow}$ values calculated from the slow decay (inverted triangles) were equal to the D_s values determined from the PDMA signal (filled circles), indicating that these signals describe the QD diffusion, which decreases with increasing PDMA concentration. At higher PDMA concentrations, both the TOPO and PDMA signals exhibit a monoexponential decay, albeit with different values of the diffusion coefficient, indicating that sufficient polymer has been added to completely displace TOPO from the QD surface.

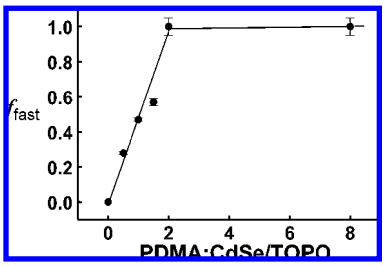

Figure 7. Fraction of TOPO displaced from CdSe/TOPO QDs (5.0 mg, 1.0×10^{-7} mol) in $CDCl_3$ by PDMA as a function of the PDMA/CdSe/TOPO weight ratio. The point at PDMA/CdSe/TOPO = 2 was measured twice to confirm that no slow component could be detected. The error bars of the first three points correspond to the standard error of the fit using eq 2. The error bars of the last two points represent the uncertainty arising from the fact that the intensities decay only to 5% of their initial values.

In Figure 7 we plot values of f_{fast} against the weight ratio of PDMA to CdSe/TOPO in the solution. The magnitude of f_{fast} increases approximately linearly with added PDMA, and we equate this value with the fraction of TOPO displaced from the particle surface. It is known that small amount of TOPO remain tightly bound to the CdSe QD surface even after exchange with PDMA.[17d] In the NMR experiment, it would be difficult to detect the contribution to diffusion of small amounts (ca. 5 wt %) of TOPO bound to the particle. Thus, we conclude conservatively that >90% of the TOPO groups on CdSe/TOPO were displaced by the polymer at a PDMA:CdSe/TOPO weight ratio of 2.0. Assuming that all PDMA molecules bind to the QDs, we deduce that, at the point of full TOPO displacement, on average 8 polymer chains bind to each QD.

Nature of the Polymer−Nanoparticle Interaction. Polymers adsorb to surfaces to form loops, trains, and tails. The term train refers to the units along the polymer backbone in direct contact with the surface. Polymer adsorption to flat surfaces is often characterized by a "pancake-to-brush" transition:[34−36] at low levels of polymer in contact with a bare surface, there is a tendency for the chains to lie flat on the surface (the pancake) with only small loops and tails. At higher levels of polymer, the adsorption density becomes much higher. Fewer segments of each chain are in contact with the surface, and repulsion between solvent swollen polymer coils forces the loops and tails to become elongated normal to the surface. These elongated chains can be thought of as a polymer brush.

The PDMA−CdSe interaction differs from this picture in several respects. First, the pronounced curvature of the surface of these very tiny nanoparticles will affect the nature of the interaction. For example, local stiffness of the polymer chain associated with finite bond lengths and rotational isomers may limit access of consecutive polymer repeat units to the surface. Second, the interaction of PDMA likely involves a specific interaction between the tertiary amine groups of the polymer and Cd atoms at the QDs surface.[37] This ligand exchange is coupled to TOPO displacement, and it is through this process

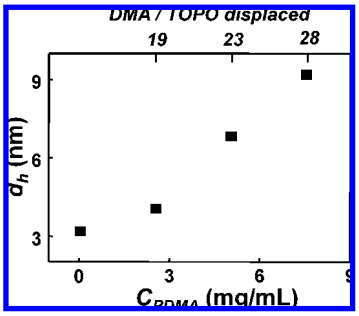

Figure 8. Calculated hydrodynamic diameter of CdSe QDs as a function of the concentration of PDMA added to the solution of CdSe/TOPO. The top axis indicates the number of PDMA units/TOPO molecule displaced, assuming that all of the PDMA is adsorbed by the QDs.

that PDMA is able to passivate the surface of the quantum dots. The PFG NMR results provide information concerning the stoichiometry of ligand exchange as well as the size of the resulting complex.

The number of DMA monomer units required to displace a single TOPO, N^*, is calculated as

$$N^* = N_{DMA}^{bound}/N_{TOPO}^{displaced} = (W_{PDMA}/M_{DMA})/(f_{fast}W_{TOPO}/M_{TOPO}) \quad (6)$$

with W_{PDMA} the weight amount of PDMA polymer added. M_{DMA} (=156) is the molecular weight of the DMA monomer; f_{fast} is the fraction of the fast component of TOPO calculated from the PFG NMR experiment. W_{TOPO} is the weight of TOPO on the CdSe/TOPO surface, and M_{TOPO} the molecular weight of TOPO (=386). The calculation yields $N^* = 19$ DMA units adsorbed to the QDs for each TOPO displaced for the case of 2.5 mg/mL of PDMA. With increasing amounts of PDMA added, the stoichiometric ratio N^* increased. Specifically, at 5.0 mg/mL PDMA, $N^* = 23$ while, at 7.5 mg/mL PDMA, $N^* = 28$.

It is known that both TOPO and amine groups coordinate Cd surface sites.[37] Assuming that one DMA unit displaces one TOPO molecule, we calculate that for the case of 2.5 mg/mL of PDMA only 4% of the PDMA groups interact directly with the CdSe surface, while the other 96% protrude into the solution. These values for all PDMA concentration are indicated on the top axis of Figure 8 and imply that the adsorbed polymer is present largely in the form of loops and tails.

In Figure 8 we also plot values of the hydrodynamic diameter of the QDs as a function of PDMA concentration, over a range where essentially all of the polymer molecules adsorb to the QDs. For example, in the presence of 2.5 mg/mL of PDMA (corresponding to an average of 2 polymer chains/particle), we note only a 30% increase in diameter. At 5.0 mg/mL PDMA (corresponding to an average of 4 polymer chains/particle), the diameter of the original particles more than doubled to 6.8 nm. Finally, at 7.5 mg/mL PDMA (corresponding to an average of 6 polymer chains/particle), d_h increased to 9.2 nm. This progressive increase of the particle diameters with added PDMA correlates with the notion that PDMA adsorbed to the QD surface adopts a conformation dominated by loops and tails extending out from the surface.

Summary

PFG NMR measurements were used to characterize the interaction of TOPO-coated CdSe QDs in $CDCl_3$ with linear PDMA with $M_n = 12\,000$ ($M_w/M_n = 1.2$, $N_n = 78$). Polymer adsorption was accompanied by displacement of TOPO molecules from the QD surface. Previous experiments have shown that ligand exchange with PDMA normally leads to a modest increase in the quantum yield of QD emission.[17b] Thus, the DMA groups of the polymer in contact with the surface are effective at passivating the surface, presumably by binding to Cd ions. At low polymer binding level, PDMA enhanced the colloidal stability of the particles but led to only a modest increase in the hydrodynamic volume of the particles. By comparing the amount of polymer added to the solution to the amount of TOPO released from the QD surface, we determined that, at lower levels of added polymer, a chain segment of on average 19 DMA monomer units was associated with the displacement of each TOPO molecule from the QD surface. We show a schematic representation of this binding process in Chart 1, where the polymer binds to the CdSe particle surface in the form of small loops.

CHART 1

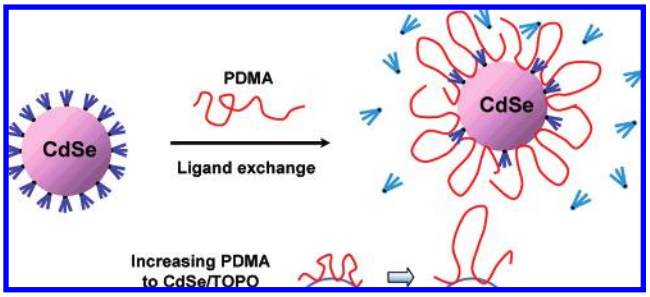

When additional polymer was added, the effective hydrodynamic diameter of the polymer increased substantially. Furthermore, an even smaller fraction of the PDMA repeat units became involved in binding to the surface as the amount of polymer adsorbed increased. At the highest level of binding, in which each nanoparticle on average had 6 polymer molecules attached, 28 DMA groups were bound for each TOPO displaced. This result indicates that, on average, only about 3% of the DMA groups interact directly with the surface, while the other 97% is present in the form of loops and tails. In Chart 1 this evolution in binding is indicated by longer loops and tails when large amounts of polymer interact with the QDs.

Taken together, these experiments emphasize how useful PFG NMR experiments are for characterizing colloidal nanocrystals in solution and for the study of their interaction with polymers.

Acknowledgment. We thank the NSERC of Canada for their support of this research. We also thank Karolina Fritz for the kind gift of PbS/OA (1109 nm) QDs and Sandeep Kumar for the CdSe/TOPO (588 nm) QDs sample, as well as Dr. John Spiro for helpful discussions.

Supporting Information Available: Pulse sequence and description of the stimulated echo (STE) pulsed field gradient (PFG) nuclear magnetic resonance (NMR) experiment, the typical STE PFG ^1H NMR spectral data set, longitudinal T_1 and transverse T_2 proton relaxation times of the TOPO terminal methyl and chain methylene segments of TOPO free in solution and bound to CdSe QDs surface, and the self-diffusion coefficient (D_s) of CdSe/TOPO QDs at various concentrations in $CDCl_3$. This material is available free of charge via the Internet at http://pubs.acs.org.

References and Notes

(1) Lee, J.; Sundar, V. C.; Heine, J. R.; Bawendi, M. G.; Jensen, K. F. *Adv. Mater.* **2000**, *12*, 1102−1105.

(2) Steckel, J. S.; Zimmer, J. P.; Coe-Sullivan, S.; Stott, N. E.; Bulović, V.; Bawendi, M. G. *Angew. Chem., Int. Ed.* **2004**, *43*, 2154−2158.
(3) Klimov, V. A.; Mikhailovsky, A. A.; Xu, S.; Malko, A.; Hollinsworth, J. A.; Leatherdale, C. A.; Eisler, H.-J.; Bawendi, M. G. *Science* **2000**, *290*, 314−317.
(4) Huynh, W. U.; Dittmer, J. J.; Alivisatos, A. P. *Science* **2002**, *295*, 2425−2427.
(5) Huynh, W. U.; Peng, X.; Alivisatos, A. P. *Adv. Mater.* **1999**, *11*, 923−923.
(6) Liu, J.; Tanaka, T.; Sivila, K.; Alivisatos, A. P.; Fréchet, J. M. *J. Am. Chem. Soc.* **2004**, *126*, 6550−6551.
(7) Schaller, R. D.; Klimov, V. I. *Phys. Rev. Lett.* **2004**, *92*, 186601.
(8) Ellingson, R. J.; Beard, M. C.; Johnson, J. C.; Yu, P.; Micic, O. I.; Nozik, A. J.; Shabaev, A.; Efros, A. L. *Nano Lett.* **2005**, *5*, 865−871.
(9) Boyenand, H.-G.; Kästle, G.; Weigl, F.; Koslowski, B.; Dietrich, C.; Ziemann, P.; Spatz, J. P.; Riethmuller, S.; Hartmann, C.; Moller, M.; Schmid, G.; Garnier, M. G.; Oelhafen, P. *Science* **2002**, *297*, 1533−1536.
(10) Narayanan, R.; El-Sayed, M. A. *Nano Lett.* **2004**, *4*, 1343.
(11) Zhou, K. B.; Wang, X.; Sun, X. M.; Peng, Q.; Li, Y. D. *J. Catal.* **2005**, *229*, 206.
(12) Han, M.; Gao, X.; Su, J. Z.; Nie, S. *Nat. Biotechnol.* **2001**, *19*, 631−635.
(13) Alivisatos, A. P. *Nat. Biotechnol.* **2004**, *22*, 47−52.
(14) Pathak, S.; Choi, S.-K.; Arnheim, N.; Thompson, M. E. *J. Am. Chem. Soc.* **2001**, *123*, 4103−4104.
(15) (a) Skaff, H.; Emrick, T. *Chem. Commun.* **2003**, *1*, 52. (b) Sill, K.; Emrick, T. *Chem. Mater.* **2004**, *16*, 1240.
(16) Potapova, I.; Mruk, R.; Prehl, S.; Zentel, R.; Basche, T.; Mews, A. *J. Am. Chem. Soc.* **2003**, *125*, 320.
(17) (a) Wang, X.; Dykstra, T. E.; Lou, X.; Salvador, M. R.; Manners, I.; Scholes, G. D.; Winnik, M. A. *J. Am. Chem. Soc.* **2004**, *126*, 7784. (b) Wang, M.; Oh, J. K.; Dykstra, T. E.; Lou, X.; Scholes, G. D.; Winnik, M. A. *Macromolecules* **2006**, *39*, 3664. (c) Wang, M.; Dykstra, T. E.; Lou, X.; Salvador, M. R.; Scholes, G. D.; Winnik, M. A. *Angew. Chem., Int. Ed.* **2006**, *45*, 2221. (d) Wang, M.; Felorzabihi, N.; Guerin, G.; Haley, J. C.; Scholes, G. D.; Winnik, M. A. *Macromolecules* **2007**, *40*, 6377.
(18) (a) Price, W. S. *Concepts Magn. Reson.* **1997**, *9*, 299−336. (b) Price, W. S. *Concepts Magn. Reson.* **1998**, *10*, 197−237. (c) Johnson, C. S., Jr. *Prog. NMR Spectrosc.* **1999**, *34*, 203−256. (d) Stilbs, P. *Prog. NMR Spectrosc.* **1987**, *19*, 1−45. (e) Kärger, J.; Pfeifer, H.; Heink, W. *Adv. Magn. Opt. Reson.* **1988**, *12*, 1−89. (f) Nicolay, K.; Braun, K. P. J.; de Graaf, R. A.; Dijkhuizen, R. M.; Kruiskamp, M. J. *NMR Biomed.* **2001**, *14*, 94−111.
(19) Terrill, R. H.; Postlethwaite, T. A.; Chen, C.; Poon, C.; Terzis, A.; Chen, A.; Hutchison, J. E.; Clark, M. R.; Wignall, G.; Londono, J. D.; Superfine, R.; Falvo, M.; Johnson, C. S., Jr.; Samulski, E. T.; Murray, R. W. *J. Am. Chem. Soc.* **1995**, *117*, 12537−12548.
(20) Kohlmann, O.; Steinmetz, W. E.; Mao, X.; Wuelfing, W. P.; Templeton, A. C.; Murray, R. W.; Johnson, C. S., Jr. *J. Phys. Chem. B* **2001**, *105*, 8801−8809.
(21) Ribot, F.; Escax, V.; Roiland, C.; Sanchez, C.; Martins, J. C.; Biesemans, M.; Verbruggen, I.; Willem, R. *Chem. Commun.* **2005**, *8*, 1019−1021.
(22) (a) Hens, Z.; Moreels, I.; Martins, J. C. *Chem. Phys. Chem.* **2005**, *6*, 2578−2584. (b) Moreels, I.; Martins, J. C.; Hens, Z. *Chem. Phys. Chem.* **2006**, *7*, 1028−1031.
(23) Murray, C. B.; Norris, D. J.; Bawendi, M. G. *J. Am. Chem. Soc.* **1993**, *115*, 8706−8715.
(24) Manna, L.; Scher, E. C.; Alivisatos, A. P. *J. Am. Chem. Soc.* **2000**, *122*, 12700.
(25) Hines, M. A.; Scholes, G. D. *Adv. Mater.* **2003**, *15*, 1844.
(26) Yu, W. W.; Qu, L.; Guo, W.; Peng, X. *Chem. Mater.* **2003**, *15*, 2854.
(27) (a) Stejskal, E. O.; Tanner, J. E. *J. Chem. Phys.* **1965**, *42*, 288−295. (b) Tanner, J. E. *J. Chem. Phys.* **1970**, *52*, 2523−2526.
(28) Fauth, J.-M.; Schweiger, A.; Braunschweiler, L.; Forrer, J.; Ernst, R. R. *J. Magn. Reson.* **1986**, *66*, 74−85.
(29) Mills, R. *J. Phys. Chem.* **1973**, *77*, 685−688.
(30) Becerra, L. R.; Murray, C. B.; Griffin, R. G.; Bawendi, M. G. *J. Chem. Phys.* **1994**, *100*, 3297−3301.
(31) Marcus, M. A.; Brus, L. E.; Murray, C. B.; Bawendi, M. G.; Prasad, A.; Alivisatos, A. P. *Nanostruct. Mater.* **1992**, *1*, 323.
(32) Kuno, M.; Lee, J. K.; Dabbousi, B. O.; Mikulec, F. V.; Bawendi, M. G. *J. Chem. Phys.* **1997**, *106*, 9869−9882.
(33) Napper, D. H. *Polymeric Stabilization of Colloidal Dispersions*; Academic Press: London, 1983; p 29.
(34) Alexander, S. *J. Phys. (Paris)* **1977**, *38*, 977−981. Alexander, S. *J. Phys. (Paris)* **1977**, *38*, 983−987.
(35) Ou-Yang, H. D.; Gao, Z. *J. Phys. 2* **1991**, *59*, 1375−1385.
(36) Charkrabati, A. *J. Chem. Phys.* **1994**, *100*, 631−635.
(37) Berrettini, M. G.; Braun, G.; Hu, J. G.; Strouse, G. F. *J. Am. Chem. Soc.* **2004**, *126*, 7063−7070.